DOI: 10.5965223811712342024739

Revista de Ciências Agroveterinárias 23 (4): 2024
Universidade do Estado de Santa Catarina

Evaluating Meteorological Drought and its Impacts on Vegetation Cover and Surface Water in the Headwater of Little Zab River Basin

Avaliação da seca meteorológica e seus impactos na cobertura vegetal e nas águas superficiais na nascente da bacia do rio Little Zab

Omeed Al-Kakey *[1(ORCID 0000-0001-6113-5994)], Volkmar Dunger [1], Mustafa Al-Mukhtar [2(ORCID 0000-0002-8850-0899)], Heman Abdulkhaleq Gaznayee [3(ORCID 0000-0002-1549-407X)]

[1]Institute of Geology, TU Bergakademie Freiberg, Freiberg, Germany. *Author for correspondence: omeed.alkakey@gmx.de
[2]University of Technology-Iraq, Baghdad, Iraq.
[3]Salahaddin University, 44002 Erbil, Iraq.

Submission: 25/07/2024 | Acceptance: 31/08/2024

ABSTRACT

Integrating information on drought incidents into planning and analysis processes can assist land, water, and urban managers to prepare more effectively for water-related hazards. This research aims to spatiotemporally assess drought characteristics upstream of the Little Zab River Basin from 2004 to 2018, merging various satellite-derived and meteorological indices to overcome gauge measurement limitations. The Coefficient of Variation (CV) was primarily utilized to investigate precipitation inconsistency on an annual timescale. The Reconnaissance Drought Index (RDI), the second Modified Soil-Adjusted Vegetation Index (MSAVI2), and the Normalized Difference Water Index (NDWI) were adopted as meteorological, agricultural, and hydrological drought indices, respectively. Ultimately, the Pearson Correlation Coefficient (PCC) statistical test was applied to comprehend the relationship between the implemented variables. Findings exhibited moderate (22.4%–28.5%) CV values in the annual precipitation data. Based on RDI_{st} results, a substantial extreme to severe drought event was recognized in the hydrological year of 2007–2008 and continued until 2008–2009 with inferior intensities at most observatories. The NDWI values displayed that the surface area of Dukan Reservoir reached its minimum extents of 133 km^2 and 123 km^2 in 2008 and 2009, respectively. Although mean MSAVI2 values competently detected the 2008 and 2009 drought incidents, those precipitation deficiencies later harmed the vegetation cover in 2010. There was a significant positive correlation between precipitation, RDI_{st}, NDWI, and mean MSAVI2 values. It is concluded that meteorological drought in the research region instantly leads to hydrological drought, resulting in agricultural drought with a one-year lag.

KEYWORDS: RDI; MSAVI2; NDWI; Kurdistan; Iraq; Iran.

RESUMO

A integração de informações sobre incidentes de seca nos processos de planeamento e análise pode ajudar os gestores da terra, da água e urbanos a prepararem-se de forma mais eficaz para os perigos relacionados com a água. Esta pesquisa tem como objetivo avaliar espaço-temporalmente as características da seca a montante da Bacia do Rio Little Zab de 2004 a 2018, combinando vários índices meteorológicos e derivados de satélite para superar as limitações de medição. O Coeficiente de Variação (CV) foi utilizado principalmente para investigar a inconsistência da precipitação em uma escala de tempo anual. O Índice de Seca de Reconhecimento (RDI), o segundo Índice de Vegetação Ajustado ao Solo Modificado (MSAVI2) e o Índice de Água por Diferença Normalizada (NDWI) foram adotados como índices de seca meteorológica, agrícola e hidrológica, respectivamente. Por fim, foi aplicado o teste estatístico Coeficiente de Correlação de Pearson (PCC) para compreender a relação entre as variáveis implementadas. Os resultados exibiram valores de CV moderados (22,4% –28,5%) nos dados anuais de precipitação. Com base nos resultados do RDI_{st}, foi reconhecido um evento substancial de seca extrema a grave no ano hidrológico de 2007-2008 e continuou até 2008-2009 com intensidades inferiores na maioria dos observatórios. Os valores do NDWI mostraram que a área superficial do reservatório de Dukan atingiu as suas extensões mínimas de 133 km^2 e 123 km^2 em 2008 e 2009, respectivamente. Embora os valores médios do MSAVI2 tenham detectado com competência os incidentes de seca de 2008 e 2009, essas deficiências de precipitação prejudicaram posteriormente a cobertura vegetal em 2010. Houve uma correlação positiva significativa entre precipitação, RDI_{st}, NDWI e valores médios de MSAVI2. Conclui-se que a seca meteorológica na região de pesquisa leva instantaneamente à seca hidrológica, resultando em seca agrícola com um atraso de um ano.

PALAVRAS-CHAVE: RDI; MSAVI2; NDWI; Kurdistan; Iraq; Iran.

INTRODUCTION

The most significant threat to humanity in the twenty-first century, along with rapid population growth, has been declared as climate change, which poses ecological systems and sustainable human and natural resource development at expanded risk (MATHBOUT et al. 2021, HAILE et al. 2020, JABBAR et al. 2020). The intense climate extremes are anticipated to alter water availability, amplify carbon releases in terrestrial habitats, and implicitly raise the quantity of water vapor in the atmosphere, thus intensifying the effects of global warming and escalating megadroughts everywhere (WANG et al. 2021). Drought is considered a natural phenomenon with multifaceted harmful impacts on humans, ecosystems, and plentiful economic divisions and is directly linked to water deficiency issues (TRAN et al. 2019). The effects of drought often develop gradually over an extended period and might persist for years even after the drought has passed; therefore, deciding the onset and end of dryness is definitively challenging (ASADI ZARCH et al. 2011). Nevertheless, a thorough drought assessment is indispensable for reducing catastrophe risks and adapting mitigation mechanisms for future growth, particularly in Arid and Semi-Arid Regions (ASARs).

With predictions of an upsurge in devastating climate extremes like drought and floods, the Middle East (ME) region has been identified as a hotspot for a drastic change in its accessible water resources and agricultural productivity (MUSTAFA ALEE et al. 2023). Even though Iraq was formerly conceived as a water-rich territory in the ME, the country has experienced disparate drought incidents over the previous decades (ALBARAKAT et al. 2022, JUMAAH et al. 2022), resulting in a complicated water dilemma that has led to population shifts, agronomic and livelihood losses, poverty escalation, and others (HASHIM et al. 2022). The Little Zab River Basin (LZRB) symbolizes a substantial transboundary watershed between Iraq and Iran, particularly the upper reaches in which the Little Zab River and smaller waterways such as Awe Shiler and Awe Gogasur originate (AL-KAKEY et al. 2023a). Apart from dryness circumstances, the LZRB was adversely affected by the construction of the Sardasht dam in Iran, resulting in a shortage of drinking and irrigation water in the majority of the province of Suleiymaniya (YOUSUF et al. 2018). Consequently, there is an urgent need to understand the interactions of climate, vegetation, and surface water upstream of LZRB.

The Coefficient of Variation (CV) is a diagnostic indicator that measures precipitation inconsistency over different timescales (LI et al. 2023), where natural disasters such as droughts and floods are more likely to occur in areas with higher precipitation variability. Besides, the Reconnaissance Drought Index (RDI) is an extensively implemented indicator for determining and projecting drought event characteristics (TSAKIRIS & VANGELIS 2005). RDI was developed to examine meteorological drought severity using two climatic parameters: Precipitation (PCP) and Potential Evapotranspiration (PET). More specifically, RDI describes the ratio of cumulative PCP to PET during a defined period, offering reliable drought assessment results (RANI et al. 2022). The Modified Soil-Adjusted Vegetation Index, in its second version (MSAVI2) (QI et al. 1994), is a spectral vegetation indicator established to cope with non-vegetated background (i.e., soil noise), predominantly in regions with sparse greenness cover (VANSELOW & SAMIMI 2014). Another important spectral indicator that complements MSAVI2 for monitoring drought dynamics is the Normalized Difference Water Index (NDWI). NDWI has been designed to recognize open water profiles (e.g., reservoir), augmenting the detection of surface water bodies while eliminating vegetation and soil characteristics (MCFEETERS 1996, ÖZELKAN 2020).

Over the past few years, several researchers have investigated and analyzed different drought categories across the Iraqi portion of LZRB. For instance, a study (AL-QURAISHI et al. 2021) in Sulaimaniyah Province applied various drought indices such as NDWI, SPI, and NDVI to evaluate drought severity and inspect changes in water bodies and plant canopy during the years 1998–2017. Results revealed that annual SPI, NDWI, and NDVI could successfully capture extreme historical droughts of 1999–2000 and 2008–2009. Another research (GAZNAYEE et al. 2022a) investigated drought intensity and frequency from 1998 to 2021 in the Kurdistan Region of Iraq (KRI) using MSAVI2, NDWI, SPI, and CV. The statistical findings of this study designated positive agreement between the applied spectral and meteorological indices. The above studies have examined agricultural, hydrological, and meteorological droughts using ground-based weather observations and satellite-derived products. However, no controlled studies have considered the northeastern part of the drainage basin (i.e., 4915 km^2) located beyond the Iraqi border due to inaccessibility to the Iranian meteorological data.

Therefore, the primary goal of this research is to provide insights into the characteristics of drought phenomenon in the headwater of LZRB from 2004 to 2018 using data acquired from weather facilities and satellite images. In this context, our ultimate objectives are to (1) explore the variability of annual precipitation over the investigated area, (2) examine meteorological drought attributes based on RDI at the selected rain gauges, (3) employ the MSAVI2 spectral indicator to assess the agricultural response to dryness events, (4)

analyze the hydrological drought of Dukan Reservoir (DR) via NDWI, and lastly (5) evaluate the implemented factors statistically and discover the agreement between them. To our knowledge, this is the first time a study combines meteorological measurements from Iraq and Iran to comprehend water deficiency in LZRB from different perspectives. The findings will likely contribute to a deeper understanding of extreme weather incidents and their reactions in such a data-scarce region.

MATERIALS AND METHODS

Study area

The region of interest characterizes the northeastern portion of LZRB that ultimately empties its surface water into Dukan Reservoir (Figure 1A). It lies between latitudes 35°24'46" N-36°54'10" N and longitudes 44°48'46" E-46°20'45" E. The investigated basin has a drainage area of 9273 km^2, of which 47% is within the Iraqi territories, and the remaining 53% is in Iran. Little Zab, the largest tributary of the Tigris River (TR), is an eighth-order river originating from the Zagros Mountains and flowing through rugged topography southwestwards until it joins TR north of Baiji, Iraq (AL-SAADY et al. 2015, AL-KAKEY et al. 2023b). The research area was chosen because it provides freshwater resources and vital agricultural outputs like barley and walnuts (AL-KAKEY et al. 2023a). The elevation in this transboundary watershed ranges from 479 m to 3577 m above sea level, and the slope gradients differ between flat and 79 degrees. Several meteorological stations are located in the examined basin, encompassing Baneh, Chwarta, Penjwen, Piranshahr, Qaladiza, and Sardasht (Figure 1A) with mean annual precipitation between 641 mm and 1057 mm through rain and snowfall (Figure 1B).

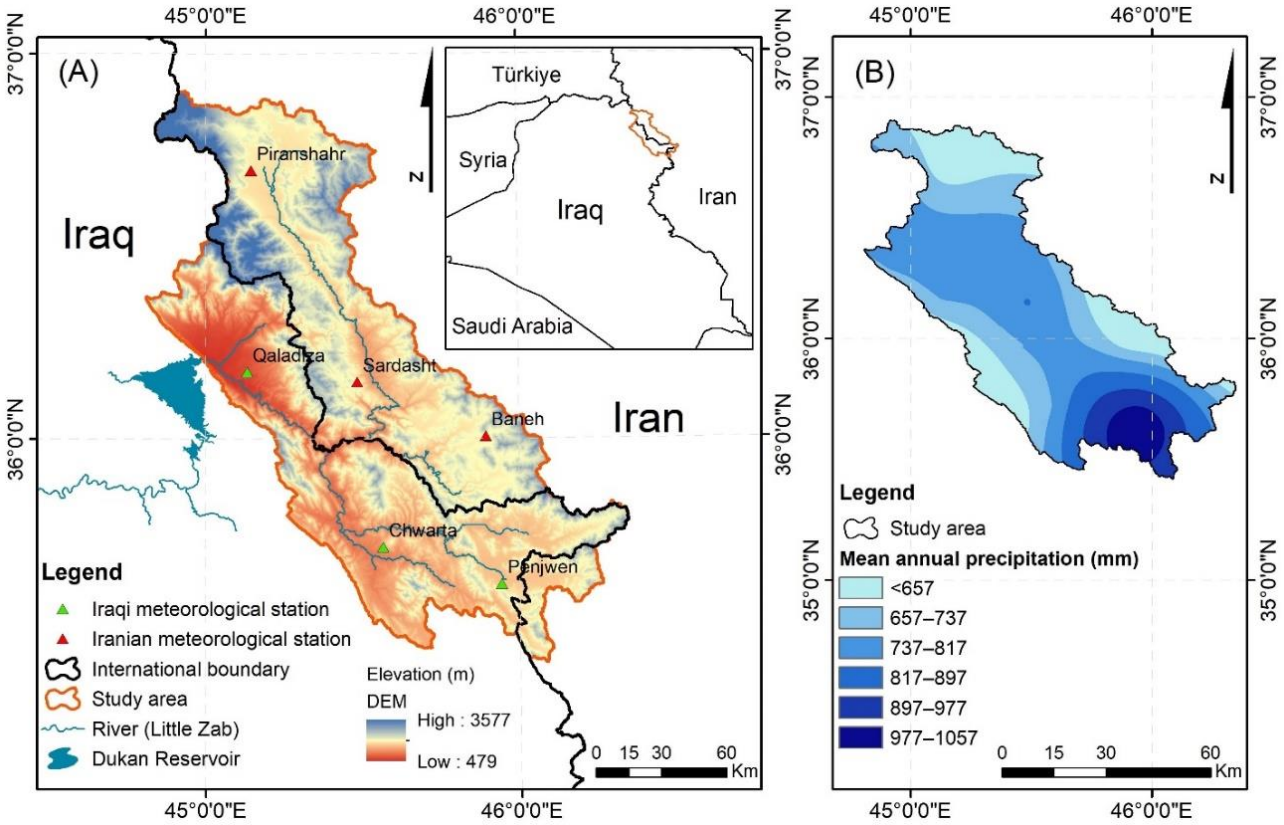

Figure 1. Location map depicting the geographical boundaries of the research region, involving the meteorological stations and Dukan Reservoir (A) and mean annual precipitation map (B).

Datasets

Acquiring in situ Meteorological Data (MD) for public use is frequently assumed to be legitimate. Nonetheless, a research trip to KRI illustrated that this is not always true. After several disappointing endeavors with the Erbil and Slemani weather bureaus, the MD was ultimately obtained from the Ministry of Agriculture and Water Resources (MAWR), KRI, covering 2004–2018. On the other hand, attaining the MD from the Iranian Meteorological Organization (IMO) was first accessible through officially authorized channels covering the period from 2004 to 2018. However, the corresponding author later attempted to obtain additional MD (2019–2023), but engagement with IMO proved fruitless due to the ongoing restrictions

against Iran. Subsequently, this study was conducted based on daily precipitation and temperature data gathered from MAWR-KRI and IMO. At last, the daily MD was converted to larger scales (i.e., monthly and annual) to evaluate precipitation variability and characterize meteorological drought incidents.

At the same time, 90 Landsat scenes were downloaded from the Landsat archives maintained on the USGS webpage (https://glovis.usgs.gov/, accessed on 01 April 2022). Furthermore, the Landsat imagery was delivered in a rectification, standardized format featuring a pixel resolution of 30 m. After that, we created a composite mosaic of six Landsat scenes for each of the 15 years to cover the entire study area. The utilized datasets were compiled from three sensors: Landsat 7 Enhanced Thematic Mapper Plus (ETM+), Landsat 5 Thematic Mapper (TM), and Landsat 8 Operational Land Imager (OLI). These datasets encompass various geographical paths and rows: 169/35, 169/34, 168/35, 168/36, 167/36, and 167/35. The Remote Sensing (RS) images were acquired between 2004 and 2018 in April and May, coinciding with the peak vegetation growth in the region of interest. In addition, the Copernicus Digital Elevation Model (CDEM) obtained from the OpenTopography website (https://opentopography.org/, accessed on 22 July 2022) with a 30 m spatial resolution was employed to delineate our study area and generate the location map. All RS datasets were consistently organized in the WGS84 datum and UTM zone 38N projection.

Coefficient of Variation (CV)

CV is an analytical metric to determine the degree of variability of precipitation data over a particular observation period, where a higher CV value corresponds with increased variability and vice versa (LI et al. 2023). According to the literature (ASFAW et al. 2018, TESFAMARIAM et al. 2019), CV categorizes the degree of variability of precipitation events into three classes: high (CV>30%), moderate (30%>CV>20%), and low (CV<20%). For this research, Equation (1) is adopted to analyze the inconsistency of annual precipitation data measured at six weather stations as follows (PAWAR et al. 2023):

$$CV = \frac{\sigma}{\bar{X}} * 100 \quad (1)$$

where σ denotes the standard deviation and $\bar{X}$ refers to the mean precipitation on an annual scale.

Reconnaissance Drought Index (RDI)

RDI emerged to tackle water shortages accurately by taking into consideration the balance between the input (i.e., precipitation) and output (i.e., potential evapotranspiration) of an aquatic system (TIGKAS et al. 2015). This study employed minimum and maximum temperatures to calculate PET values using the empirical Hargreaves method, which proved its superiority in mountainous areas compared to other approaches such as Blaney–Criddle and Thornthwaite (ABUBAKAR et al. 2020). Three forms of RDI are presented in the literature: the initial (a_k), the normalized (RDI_n), and the standardized (RDI_{st}) (TIGKAS et al. 2017). The average annual a_k can be exploited as the Aridity Index (AI) at a given location (TIGKAS 2008). In contrast, the standardized RDI can calculate drought severity (MOHAMMED & SCHOLZ 2018). Hence, the initial value (a_k) of RDI is computed in the Drought Indices Calculator (DrinC) software (version 1.7) following Equation (2) (TIGKAS et al. 2013):

$$a_k^i = \frac{\sum_{j=1}^{k} PCP_{ij}}{\sum_{j=1}^{k} PET_{ij}}, i = 1(1)N \; and \; j = 1(1)k \quad (2)$$

where PCP_{ij} and PET_{ij}, respectively, symbolize precipitation and potential evapotranspiration of the *i*-th hydrological year (October-September) and the *j*-th month, and *N* denotes the sum of all hydrological years for the relevant climate.

The RDI_{st} values can be classified into eight categories (Table 1), and Equation (3) is applied in DrinC for the calculation of RDI_{st} as follows (TIGKAS et al. 2013):

$$RDI_{st}^i = \frac{y^i - \bar{y}}{\hat{\sigma}_y} \quad (3)$$

where y^i signifies the $\ln(a_k^i)$, $\bar{y}$ stands for its arithmetic mean, and $\hat{\sigma}_y$ refers to its related standard deviation.

Table 1. Classification of dry and wet conditions based on RDI_{st} values (TIGKAS 2008).

RDI_{st} Value	Dryness/Wetness Category
–2.0 or less	Extreme Dryness
–1.99 to –1.50	Severe Dryness

–1.49 to –1.0	Moderate Dryness
–0.99 to 0	Normal (Mild) Dryness
0 to 0.99	Normal (Mild) Wetness
1.0 to 1.49	Moderate Wetness
1.5 to 1.99	Severe Wetness
2.0 or more	Extreme Wetness

Second Modified Soil-Adjusted Vegetation Index (MSAVI2)

MSAVI2 is a spectral vegetation index designed to deliver precise data for territories with little greenery or canopy plants with low levels of chlorophyll. It aims to detect the exposed soil between seedlings more accurately during leaf growth, which is advantageous for agricultural monitoring (LEMENKOVA & DEBEIR 2023). Furthermore, MSAVI2 can be used for mapping terrains with a substantial portion of bare surfaces, where its spatial behavior provides solid evidence for land categorization (MARZIALETTI et al. 2020). An earlier study (GAZNAYEE & AL-QURAISHI 2019) determined that utilizing MSAVI2 and its derivatives and transformations can significantly improve drought monitoring. In terms of the numerical scale, MSAVI2 values range between −1 (bare surface) and +1 (vegetative land); higher values denote higher photosynthetic biomass percentages (GAZNAYEE et al. 2022a). In this study, MSAVI2 is calculated per pixel in the Google Earth Engine (GEE) using Equation (4) (VICARIO et al. 2019):

$$MSAVI2 = \frac{2NIR + 1 - \sqrt{(2NIR + 1)^2 - 8(NIR - RED)}}{2} \quad (4)$$

where *NIR* refers to the Near-InfraRed band and *RED* implies the Red band of spaceborne images.

Normalized Difference Water Index (NDWI)

According to MCFEETERS (1996), NDWI is a remotely sensed tool to distinguish and delineate open water features (e.g., lakes, rivers, and deltas) and improve their presence in satellite imagery. NDWI is also designed to offer researchers estimates of the turbidity of water masses using RS data. Water bodies could be depicted by applying a threshold value that differentiates between landscapes (NDWI values below 0.3) and water surfaces (NDWI values above or equal to 0.3) (GAZNAYEE et al. 2022a). Thus, the Green and NIR bands of satellite imagery are utilized for this research in ERDAS Imagine 2015 to compute NDWI for DR following Equation (5) (AL-QURAISHI et al. 2021, LEMENKOVA & DEBEIR 2023):

$$NDWI = \frac{(Green - NIR)}{(Green + NIR)} \quad (5)$$

where *Green* indicates the green band and *NIR* signifies the Near-InfraRed band of earth observation imagery.

Statistical measure

Pearson proposed the Pearson Correlation Coefficient (PCC) (PEARSON 1895), which has been extensively applied in scientific studies (ZHOU et al. 2021). It is one of the most frequently employed statistical measures for assessing the relationships between drought indices (HANADÉ HOUMMA et al. 2023). In the PCC matrix, the values theoretically range from +1 to –1, wherein the signs demonstrate the direction and strength of the linear relationship between variables (GAZNAYEE et al. 2022b, ZHOU et al. 2021). Further, +1 implies a perfect positive linear connection between variables, –1 specifies a perfect negative linear correlation, and zero values denote no linear relationship (RATNER 2009). Similar to several earlier research (AL-QURAISHI 2021, GAZNAYEE et al. 2022a, GAZNAYEE & AL-QURAISHI 2019), the PCC matrix is implemented for this study to compare the response time among various drought types (i.e., meteorological, hydrological, and agricultural) from a linear perspective. The XLSTAT add-on is used to create the PCC matrix for the present investigation.

RESULTS

Assessment of precipitation variability

The current work implemented CV to gain insight into the dynamical patterns of precipitation inconsistency over the region of interest during the study period. Based on the Mean Annual Precipitation (MAP) data, the CV values were calculated at each of the six meteorological stations, as depicted in Figure 2. Precipitation data from all rain gauges showed moderate variability (i.e., 30%>CV>20%). Moreover, the analysis results indicate that Qaladiza station, with a CV of 28.5%, exhibited the most augmented precipitation irregularity from 2004 to 2018, whereas Sardasht station displayed the least, with a CV of 22.4%. Similarly, Penjwen and Baneh stations documented the highest and lowest MAP of 1057 mm and

641 mm, respectively. Notably, the maximum CV value is perceived near the outlet of the research basin, which is relatively situated at the lowest elevation, 628 m above sea level. In sharp contrast, the minimum CV value was measured in the center of the watershed. The southeastern ranges of the study area, which characterize the highest precipitation records, demonstrated CV values comparable to those of the northern part. Besides, precipitation noticeably diminishes towards the southwestern zone of the river basin.

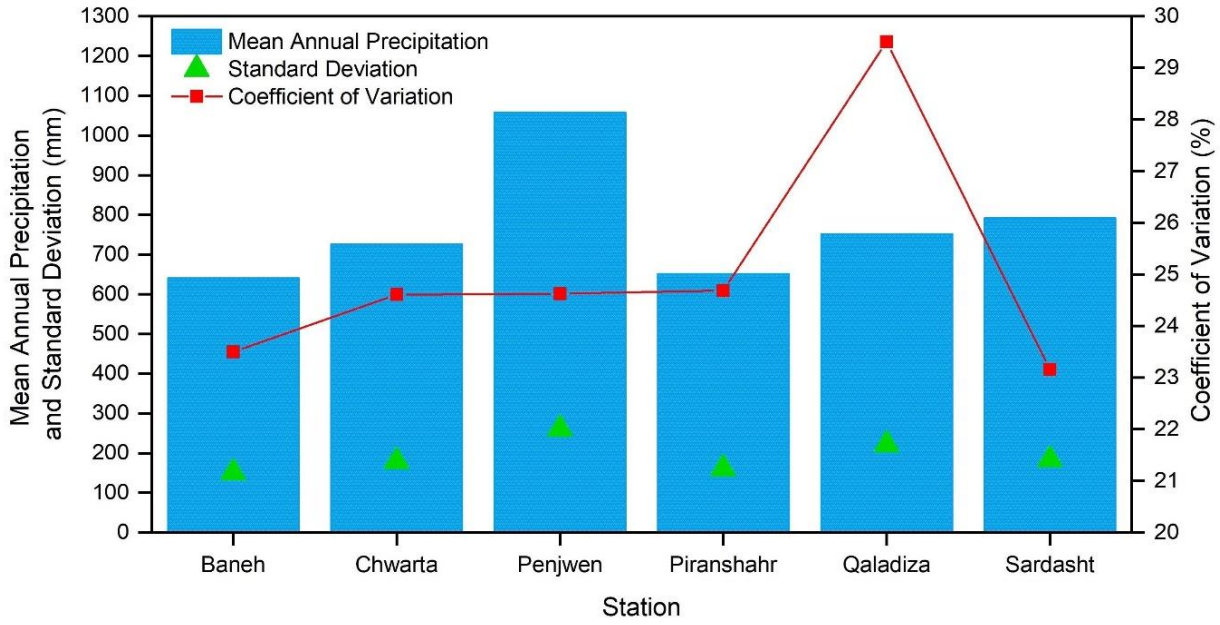

Figure 2. Descriptive statistics of MAP measured from 2004 to 2018 at the six rain gauges.

Evaluation of RDI_{st}

RDI_{st}, as a meteorological indicator, was calculated for the weather station records in LZRB on an annual temporal scale, utilizing precipitation and temperature data spanning from 2004 to 2018. As exposed in Figure 3, the implemented index has different evolutions from station to station. Nonetheless, the hydrological year of 2007–2008 witnessed an extreme drought incident at most observatories, except Chwarta, which encountered less intense drought circumstances during the same year. Furthermore, stations like Penjwen, Chwarta, and Sardasht distinguished mutual moderate drought of varying lengths in 2008–2009, whereas Chwarta and Sardasht observed second moderate dryness in the years 2012–2013 and 2013–2014, respectively. At Piranshahr station, which is positioned at a distinctive elevation of 1444 m above sea level, severe dryness was noted in 2016–2017. Despite this, 2015–2016 recorded moderate to severe wetnesses across all observational facilities under investigation. Based on RDI_{st} results, the driest year in the study area was 2007–2008, with an average value of −2.19, sustained as a mild drought event in 2008–2009, with an average value of −0.79. In contrast, the wettest year, with an average value of 1.60, was documented in 2015–2016.

It can be inferred that the frequencies of normal dryness are higher than those of other drought categories at the six meteorological stations, as exposed in Figure 3. This finding indicates a maximum likelihood of mild droughts occurring or returning in the study area. Aside from the driest and wettest years, the available data indicate an erratic seasonal pattern of rainy and dry intervals across the fifteen years under investigation. In addition to RDI_{st}, the precipitation and temperature data were utilized in DrinC as primary inputs to calculate the AI value at each of the six meteorological stations, ultimately categorizing the entire research area into three distinct climate zones: dry-subhumid (Baneh, Chwarta, and Piranshahr), humid (Penjwen and Sardasht), and semi-arid (Qaladiza) during the exploration period.

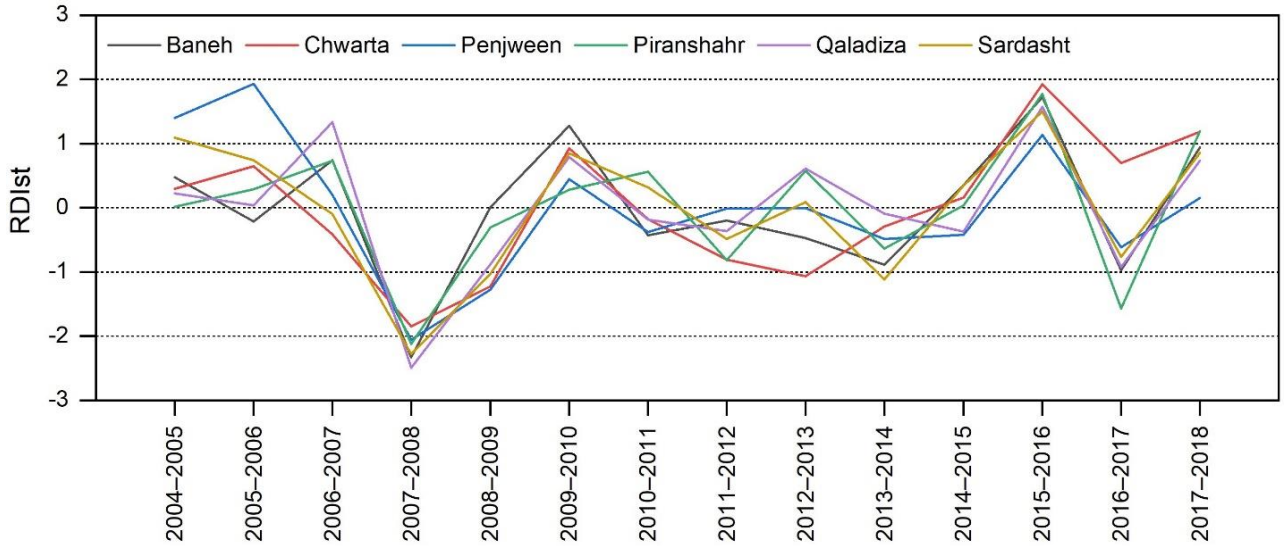

Figure 3. Time series of annual RDI_{st} for the selected meteorological stations from 2004 to 2018.

Analysis of MSAVI2

The MSAVI2 values were computed for this research in GEE using spectral reflectance values of NIR and RED bands of satellite imagery. Figure 4 visually represents the calculated MSAVI2 for the explored region from 2004 to 2018. On a numerical scale, the values of MSAVI2 span between −1 and +1, where a higher value indicates a more significant percentage of photosynthetic biomass. It is worth perceiving that characteristics other than vegetation, such as built-up lands, barren surfaces, and water bodies, are indicated by MSAVI2 values between −1 and zero (AZADI et al. 2022). The mean values of MSAVI2 and vegetation cover in square kilometers are also displayed in Figure 4. The results exhibited that the lowest mean values of MSAVI2 for 2008 and 2009 were 0.14 and 0.15, respectively. These small values instantly correspond to a decline in the quantity of annual precipitation. In contrast, the highest mean value of 0.40 was attained in 2016, signifying healthy and abundant vegetation. Even though the mean values of MSAVI2 substantially responded to the fluctuations in mean annual precipitation, the territory inhabited by greenery reacted to the drought incidents of 2008 and 2009 with a time lag. In other words, the lowest MAP of 503 mm was observed in 2008, indicating extreme dryness; however, the plant cover was harmfully affected and reached its minimum extension of 3678 km^2 in 2010.

Analysis of NDWI

According to the assessment of NDWI values, the surface area of Dukan Reservoir significantly dropped to its smallest extents of 133 km^2 and 123 km^2 in 2008 and 2009, respectively. On the flip side, the artificial lake reached its largest dimensions of 251 km^2, 234 km^2, 227 km^2, and 222 km^2 in 2004, 2005, 2016, and 2017, respectively (Figure 5). While Dukan dam administration primarily controls the volume of water in Dukan Reservoir, climatological variables such as inconstancy in precipitation also have a meaningful role in quantifying the water body. Thus, it is evident that there is a strong correlation between the drastic reduction in the surface area of DR during the years 2008 and 2009 and the annual precipitation deficiency (i.e., drought events) in those years.

Statistical assessment

The PCC matrix was employed in this investigation to provide insight into any possible connection between the variables utilized for drought characterization in the upper reaches of LZRB. The correlation coefficient analysis between mean annual precipitation, drought indices, as well as additional explanatory components was conducted in XLSTAT. As revealed in Table 2, RDI_{st} unsurprisingly showed a solid positive relationship with MAP, where precipitation data signify a major input in calculating the reconnaissance drought index. Simultaneously, CV had a weak positive correlation with mean annual precipitation. Even though the relationship between MAP and mean MSAVI2 values was positive and very strong, terrains covered by vegetation exhibited a negligible relationship with mean annual precipitation. The surface area of Dukan Reservoir responded to MAP, RDI_{st}, CV, and mean MSAVI2 values with a robust positive correlation. Nevertheless, it was evident that the water body and the plant coverage have no instant connection. Contrary to that, mean MSAVI2 values displayed strong to very strong positive correlations with all variables, aside from vegetation cover, as mentioned previously. It may be inferred that the correlation between MSAVI2, NDWI, and the meteorological variables provided significant new information on the fundamental dynamics of vegetation pattern change over time in this mountainous watershed.

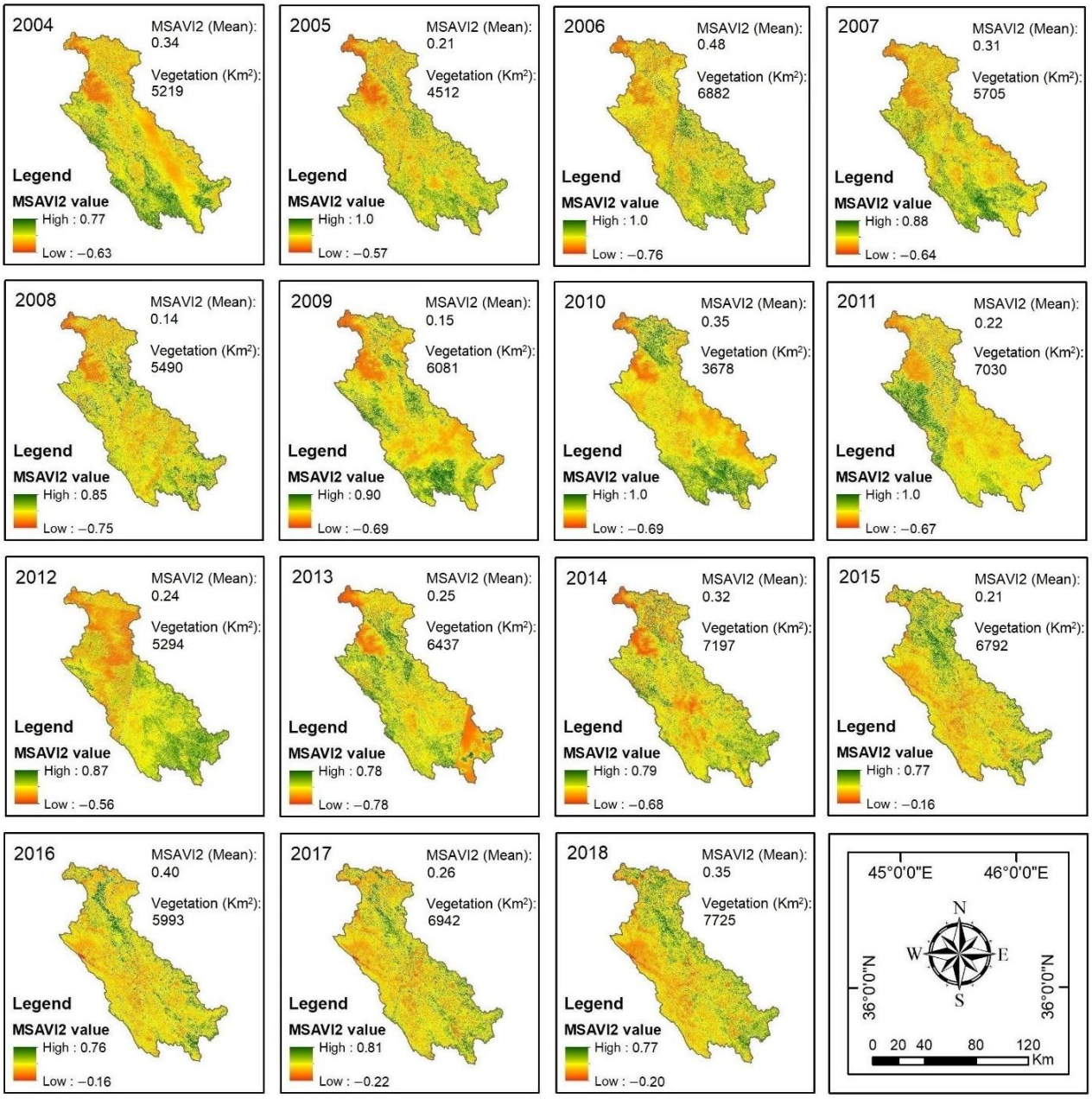

Figure 4. Detecting vegetation cover changes based on MSAVI2 in the investigated basin.

Figure 5. Areal changes to Dukan Reservoir based on NDWI between 2004 and 2018.

Table 2. Pearson correlation matrix of the implemented variables for drought characterization.

Variable	MAP (mm)	RDI_{st}	CV (%)	MSAVI2 (Mean)	Vegetation (Km^2)	DR Area (Km^2)
MAP (mm)	1	0.982*	0.295	0.756*	−0.037	0.586*
RDI_{st}	0.982*	1	0.292	0.699*	−0.064	0.591*
CV (%)	0.295	0.292	1	0.558*	−0.074	0.563*
MSAVI2 (Mean)	0.756*	0.699*	0.558*	1	0.179	0.539*
Vegetation (Km^2)	−0.037	−0.064	−0.074	0.179	1	0.032
DR Area (Km^2)	0.586*	0.591*	0.563*	0.539*	0.032	1

* Correlation is significant at the alpha level of 0.05.

DISCUSSION

As stated in the literature review, the lack of Iranian meteorological data hindered prior studies (AL-QURAISHI 2021, GAZNAYEE et al. 2022a) from thoroughly investigating drought phenomena in the northeastern portion of the drainage basin beyond the Iraqi border, which encompasses a massive area of 4915 km^2. In these circumstances, the current research attempted to fill this substantial gap by acquiring daily meteorological measurements from Iraq and Iran and RS images to assess dryness characteristics in

the headwater region of LZRB from diverse viewpoints. Primarily, this study evaluated the inconsistency of annual precipitation utilizing the coefficient of variation. The present study also inspected meteorological drought attributes from 2004 to 2018 based on RDI. Alongside, agricultural and hydrological drought incidents in the Little Zab River Basin were analyzed using the MSAVI2 and NDWI spectral indices. The PCC matrix was eventually applied to comprehend the connections between utilized factors. Noticeably, a significant positive correlation existed between mean annual precipitation, RDI_{st}, mean MSAVI2 values, and the surface area of DR.

To deeply understand how precipitation deficiencies affected upstream of LZRB, we examined the degree of precipitation variability from the annual perception in this research. All meteorological stations revealed moderate precipitation variation ranging from 22.4% to 28.5%. The lowest CV value of MAP was determined in the middle of the watershed, whereas the southwestern part of the basin had the most significant fluctuation in precipitation with the lowest elevation of 628 m. Therefore, it can be inferred that the variability in annual precipitation increases as elevation declines, mainly in the direction of the southwestern range of LZRB. Since extreme events such as droughts and floods are more likely to occur in territories that experience more significant rainfall variability (MCKEE et al. 1993), such spatial examination of the CV values is essential to predominately understand the risk of abnormal climate conditions in the research basin.

To this end, based on the applied meteorological index, which demonstrates its appropriateness for identifying drought characteristics, this research revealed that RDI_{st} has a non-uniform cyclic pattern of dry and wet intervals from station to station (Figure 3). However, the driest hydrological year at all investigated observatories was 2007–2008, with an average RDI_{st} value of −2.19, tracked by a mild drought event in 2008–2009, with a value of −0.79. On the contrary, the most significant wet year was 2015–2016. Remarkably, it was evident that mild dryness prevailed across the region of interest. This research supports evidence from previous studies conducted in the KRI (AL-QURAISHI et al. 2021, GAZNAYEE et al. 2022a) regarding historical drought incidents.

The MSAVI2 indicator derived from RS imagery was used in this investigation to detect changes in vegetation cover in response to drought occurrences from 2004 to 2018. Findings showed that, for the years 2008 and 2009, the lowest mean values of MSAVI2 were 0.14 and 0.15, respectively. These low numbers indicate a substantial reduction in the amount of precipitation that falls during the year. Although the mean MSAVI2 measurements significantly responded to precipitation variations, the vegetation cover gradually adapted to the 2008 drought event. Put another way, the impact of consecutive drought events of 2008 and 2009 was observed later in 2010 when the plant cover shrank to its minimum extension. This outcome suggests that short-term precipitation deficits have little impact on vegetation areas upstream of the Little Zab River Basin. It is encouraging to compare our result with that reported by AL-QURAISHI et al. (2021), who discovered that plant canopy in the Iraqi part of LZRB (Sulaimaniyah Province) reacts to precipitation shortage with a one-year lag.

Several factors could explain this time lag between precipitation deficiency and vegetation cover response. Firstly, this could be attributed to the considerable percentage of natural vegetation that prevails upstream of LZRB, such as bushes, trees, perennial plants, and orchards that deliver a variety of nuts and fruits (AL-SAADY et al. 2015), where, in general terms, vegetation categorized under forestry is less sensitive to changes in precipitation than grassland (PETRAKIS et al. 2016). Another feasible cause is the snowmelt waters, which can provide aquatic demands for plant growth during dry years. Previous research (GAZNAYEE et al. 2022a) found that successive drought incidents harshly affected the vegetation cover of the Iraqi Kurdistan Region. Furthermore, the successive dry years induced the overgrazing of livestock breeders towards the mountainous territories and disrupted the physiological cycle of seed formation.

Another spectral index used herein was NDWI, which was employed to delineate the surface area of Dukan Reservoir and calculate alterations that occurred between 2004 and 2018. As shown in Figure 5, the reservoir area profoundly decreased, reaching its minimum dimensions of 133 km^2 and 123 km^2 in 2008 and 2009, respectively. This finding agrees with the results of RDI_{st}, which indicated moderate to extreme meteorological drought events in the years 2007–2008 and 2008–2009. It can be claimed that shrinkages in the reservoir area were instantly and tightly connected with mean annual precipitation deficiencies. This result also accords with an earlier study (GAZNAYEE et al. 2022a), which disclosed that the reservoir area witnessed considerable reductions in 2008 and 2009. In general, the Tigris–Euphrates basin encountered an extensive drop in its total water storage by approximately 93 km^3 during the 2007–2009 drought period (LONGUEVERGNE et al. 2013). It is worth noting that several internal and external factors determine the water capacity of Dukan Reservoir, such as water management strategies in Iran (e.g., Sardasht dam) (YOUSUF et al. 2018), precipitation variability over the region, as well as water demands in the middle and

southern Iraq.

Despite these promising outcomes, additional studies are still required to implement long-term climatological databases such as FLDAS, SPEI, and ERA5-Land (ALBARAKAT et al. 2022, MUSTAFA ALEE et al. 2023, MUÑOZ-SABATER et al. 2021), which can systematically inspect the repercussions of drought events in the area of interest. Nonetheless, the reliability of such products must be sufficiently examined, particularly in basins characterized by vast climate variations. Further investigations are needed to understand the driving mechanisms that affect annual precipitation fluctuations, such as regional climate patterns, management practices, and land use changes. Developing an early warning system for drought surveillance via geospatial technologies could be possible in upcoming studies. Future research must also move toward a greater variety of drought-resistant plant species to mitigate the effects of water shortages.

CONCLUSION

This research aimed to assess the feasibility of integrating ground-based meteorological data and satellite images to characterize drought phenomena upstream of LZRB. The present study discovered that all rain gauges experienced moderate CV values ranging from 22.4% to 28.5% on the annual timescale. Consequently, in contrast to expectations, we found that this mountainous basin underwent erratic precipitation between 2004 and 2018, manifesting as drought incidents. Furthermore, it was evident that precipitation instability increased toward the southwestern part of LZRB, representing Qaladiza with the lowest elevation. One of the more significant conclusions from this research is that the meteorological drought in the study area immediately caused hydrological drought; nonetheless, it resulted in agricultural drought with a one-year lag. These findings highlight the importance of combining diverse datasets to analyze and comprehend the relationship between water availability and plant conditions in areas with little data. Therefore, this study could assist policymakers in developing early warning systems and drought monitoring strategies to mitigate the adverse impact of climate extremes.

ACKNOWLEDGEMENTS

The authors are grateful to all data providers mentioned in the “Datasets” section. Appreciation also goes to the German Academic Exchange Service for funding this research (grant number 57381412). Lastly, we thank the editor and anonymous reviewers for their insightful comments and recommendations.

REFERENCES

ABUBAKAR HB et al. 2020. Drought characterization and trend detection using the reconnaissance drought index for setsoto municipality of the free state province of south africa and the impact on maize yield. Water 12: 1–16.

AL-KAKEY O et al. 2023a. Proposing Optimal Locations for Runoff Harvesting and Water Management Structures in the Hami Qeshan Watershed, Iraq. ISPRS International Journal of Geo-Information 12: 312.

AL-KAKEY O et al. 2023b. Assessing CFSR climate data for rainfall-runoff modeling over an ungauged basin between Iraq and Iran. Kuwait Journal of Science 50: 405–414.

AL-QURAISHI AMF et al. 2021. Drought trend analysis in a semi-arid area of Iraq based on Normalized Difference Vegetation Index, Normalized Difference Water Index and Standardized Precipitation Index. Journal of Arid Land 13: 413–430.

AL-SAADY Y et al. 2015. Land use and land cover (LULC) mapping and change detection in the Little Zab River Basin (LZRB), Kurdistan Region, NE Iraq and NW Iran. Freiberg Online Geoscience 43: 1–32.

ALBARAKAT R et al. 2022. Assessment of drought conditions over Iraqi transboundary rivers using FLDAS and satellite datasets. Journal of Hydrology: Regional Studies 41: 101075.

ASADI ZARCH MA et al. 2011. Drought Monitoring by Reconnaissance Drought Index (RDI) in Iran. Water Resources Management 25: 3485–3504.

ASFAW A et al. 2018. Variability and time series trend analysis of rainfall and temperature in northcentral Ethiopia: A case study in Woleka sub-basin. Weather and Climate Extremes 19: 29–41.

AZADI S et al. 2022. The Gavkhouni Wetland Dryness and Its Impact on Air Temperature Variability in the Eastern Part of the Zayandeh-Rud River Basin, Iran. Water 14: 172.

GAZNAYEE HAA et al. 2022a. Drought Severity and Frequency Analysis Aided by Spectral and Meteorological Indices in the Kurdistan Region of Iraq. Water 14: 3024.

GAZNAYEE HAA et al. 2022b. A Geospatial Approach for Analysis of Drought Impacts on Vegetation Cover and Land Surface Temperature in the Kurdistan Region of Iraq. Water 14: 927.

GAZNAYEE HAA & AL-QURAISHI AMF 2019. Analysis of Agricultural Drought, Rainfall, and Crop Yield Relationships in Erbil Province, the Kurdistan Region of Iraq based on Landsat Time-Series MSAVI2. Journal of Advanced Research in Dynamical and Control Systems 11: 536–545.

HAILE GG et al. 2020. Projected Impacts of Climate Change on Drought Patterns Over East Africa. Earth’s Future 8: 1–23.

HANADÉ HOUMMA I et al. 2023. A new multivariate agricultural drought composite index based on random forest algorithm and remote sensing data developed for Sahelian agrosystems. Geomatics, Natural Hazards and Risk 14: 2223384.

HASHIM BM et al. 2022. Assessment of Future Meteorological Drought Under Representative Concentration Pathways (RCP8.5) Scenario: Case Study of Iraq. Knowledge-based Engineering and Sciences 3: 64–82.

JABBAR A et al. 2020. Change detection of glaciers and snow cover and temperature using remote sensing and GIS: A case study of the Upper Indus Basin, Pakistan. Remote Sensing Applications: Society and Environment 18: 100308.

JUMAAH HJ et al. 2022. Monitoring and evaluation Al-Razzaza lake changes in Iraq using GIS and remote sensing technology. The Egyptian Journal of Remote Sensing and Space Sciences 25: 313–321.

LEMENKOVA P & DEBEIR O 2023. Computing Vegetation Indices from the Satellite Images Using GRASS GIS Scripts for Monitoring Mangrove Forests in the Coastal Landscapes of Niger Delta, Nigeria. Journal of Marine Science and Engineering 11: 871.

LI Z et al. 2023. Diurnal Variation Characteristics of Summer Precipitation and Related Statistical Analysis in the Ili Region, Xinjiang, Northwest China. Remote Sensing 15: 3954.

LONGUEVERGNE L et al. 2013. GRACE water storage estimates for the Middle East and other regions with significant reservoir and lake storage. Hydrology and Earth System Sciences 17: 4817–4830.

MARZIALETTI F et al. 2020. Mapping Coastal Dune Landscape through Spectral Rao's Q Temporal Diversity. Remote Sensing 12: 2315.

MATHBOUT S et al. 2021. Mediterranean-Scale Drought: Regional Datasets for Exceptional Meteorological Drought Events during 1975–2019. Atmosphere 12: 941.

MCFEETERS SK. 1996. The use of the Normalized Difference Water Index (NDWI) in the delineation of open water features. International Journal of Remote Sensing 17: 1425–1432.

MCKEE TB et al. 1993. The Relationship of Drought Frequency and Duration to Time Scales. Proceedings of the Eighth Conference on Applied Climatology 1–6.

MOHAMMED R & SCHOLZ M 2018. Flow–duration curve integration into digital filtering algorithms for simulating climate variability based on river baseflow. Hydrological Sciences Journal 63: 1558–1573.

MUÑOZ-SABATER J et al. 2021. ERA5-Land: a state-of-the-art global reanalysis dataset for land applications. Earth System Science Data 13: 4349–4383.

MUSTAFA ALEE M et al. 2023. Drought Assessment across Erbil Using Satellite Products. Sustainability 15: 6687.

ÖZELKAN E. 2020. Water Body Detection Analysis Using NDWI Indices Derived from Landsat-8 OLI. Polish Journal of Environmental Studies 29: 1759–1769.

PAWAR U et al. 2023. Spatiotemporal Rainfall Variability and Trends over the Mahi Basin, India. Climate 11: 163.

PEARSON K 1895. VII. Note on regression and inheritance in the case of two parents. Proceedings of the Royal Society of London 58: 240–242.

PETRAKIS R et al. 2016. Vegetative response to water availability on the San Carlos Apache Reservation. Forest Ecology and Management 378: 14–23.

QI J et al. 1994. A modified soil adjusted vegetation index. Remote Sensing of Environment 48: 119–126.

RANI A et al. 2022. Spatio-temporal assessment of agro climatic indices and the monsoon pattern in the Banas River Basin, India. Environmental Challenges 7: 100483.

RATNER B 2009. The correlation coefficient: Its values range between +1/−1, or do they?. Journal of Targeting, Measurement and Analysis for Marketing 17: 139–142.

TESFAMARIAM BG et al. 2019. Characterizing the spatiotemporal distribution of meteorological drought as a response to climate variability: The case of rift valley lakes basin of Ethiopia. Weather and Climate Extremes 26: 100237.

TIGKAS D 2008. Drought Characterisation and Monitoring in Regions of Greece. European Water 23: 29–39.

TIGKAS D et al. 2013. The RDI as a composite climatic index. European Water 41: 17–22.

TIGKAS D et al. 2015. DrinC: a software for drought analysis based on drought indices. Earth Science Informatics 8: 697–709.

TIGKAS D et al. 2017. An Enhanced Effective Reconnaissance Drought Index for the Characterisation of Agricultural Drought. Environmental Processes 4: 137–148.

TRAN T et al. 2019. Assessing Spatiotemporal Drought Dynamics and Its Related Environmental Issues in the Mekong River Delta. Remote Sensing 11: 2742.

TSAKIRIS G & VANGELIS H 2005. Establishing a drought index incorporating evapotranspiration. European Water 9: 3–11.

VANSELOW K & SAMIMI C 2014. Predictive Mapping of Dwarf Shrub Vegetation in an Arid High Mountain Ecosystem Using Remote Sensing and Random Forests. Remote Sensing 6: 6709–6726.

VICARIO S et al. 2019. Bayesian Harmonic Modelling of Sparse and Irregular Satellite Remote Sensing Time Series of Vegetation Indexes: A Story of Clouds and Fires. Remote Sensing 12: 83.

WANG M et al. 2021. Divergent responses of ecosystem water-use efficiency to extreme seasonal droughts in Southwest China. Science of The Total Environment 760: 143427.

YOUSUF MA et al. 2018. Sustainable Water Management in Iraq (Kurdistan) as a Challenge for Governmental Responsibility. Water 10: 1651.

ZHOU Z et al. 2021. Investigating the Propagation From Meteorological to Hydrological Drought by Introducing the Nonlinear Dependence With Directed Information Transfer Index. Water Resources Research 57: 1–21.